294 J. Chem. Eng. Data 1986, 31, 294-296

Solubility of Hydrogen in Methanol Containing Reaction Species for Hydrogenation of *o*-Nitrophenol

Vasant R. Choudhary,* Mukund G. Sane, and Hemant G. Vadgaonkar

Chemical Engineering Division, National Chemical Laboratory, Pune 411 008, India

The solubility of hydrogen in methanol in the presence of *o*-nitrophenol, *o*-aminophenol, and water at different temperatures (293–328 K) and pressures (439–2145 kPa) has been determined. The presence of the above species caused a significant decrease in the solubility. The dissolution of hydrogen was found to be an endothermic process.

Introduction

Precise data on the solubility of a gas, which is one of the reactants, is required in interpreting the kinetics of gas–liquid and gas–liquid–solid (catalytic or noncatalytic) reactions. However, it is necessary to know not only the solubility of the gas in the solvent used as a reaction medium, but also the solubility of the gas in the presence of reaction species in the medium. It is not easy to estimate the solubility of a gas in the reaction mixture directly from the solubility data for the gas–solvent system and hence it must be measured experimentally.

Our earlier studies on the hydrogenation of *o*-nitrophenol on Pd–carbon indicated that methanol is the best reaction medium among the C_1–C_4 alcohols for the hydrogenation. The solubility of hydrogen in methanol at different pressures and temperatures has already been reported (*1*, *2*). Recent studies (*3*–*5*) have shown that the solubility of hydrogen in methanol is strongly affected by the presence of *o*-nitroanisole (*3*), nitrobenzene (*4*), and *p*-nitrotoluene (*5*). The present work was undertaken with the objective of collecting the data on the solubility of hydrogen in methanol containing reaction species for the hydrogenation of *o*-nitrophenol (viz., *o*-nitrophenol, *o*-aminophenol, and water) at different pressures and temperatures; the data was necessary for modelling of the hydrogenation reaction in a three-phase slurry reactor.

Experimental Section

The solubility of hydrogen in pure methanol and methanol containing the reaction species, individually and in their mixture, at the concentrations that are involved in the hydrogenation was determined by using the solubility apparatus described earlier by Choudhary et al. (*6*) and later used by Radhakrishnan et al. (4). In order to study the effect of temperature and pressure, the temperature was varied from 293 to 328 K and the pressure from about 439 to 2145 kPa. These ranges of pressure and temperature cover the process variables for the hydrogenation.

The reaction medium (1000 cm^3 of methanol with or without the reaction species) was first degassed and then saturated with high-purity hydrogen (>99.99%) in a stirred Parr autoclave (made of 316 stainless steel; capacity, 2000 cm^3; inside diameter, 10 cm; inside depth, 26.7 cm) at the required temperature and pressure. The reaction medium was stirred at a stirring speed of 760 rpm by a turbine stirrer (diameter 5.5 cm, situated at a distance of 2.8 cm from the bottom of the autoclave) while maintaining the pressure of hydrogen constant. The saturation was carried out for a period of 1 h. After the saturation, a known amount of the saturated liquid sample was transferred in to a gas buret, where the dissolved hydrogen was desorbed at atmospheric pressure. The desorbed hydrogen ranging from 10 to 20 cm^3 (STP) was collected over methanol, which was presaturated with hydrogen, and measured quantitatively. A detailed description of the apparatus and the experimental procedure is given in ref *6*.

Table I. Data on Solubility of Hydrogen in Methanol Containing Reaction Species at Different Concentrations

temp, K	press., kPa	solubility, s, $\mu mol \cdot cm^{-3} \cdot kPa^{-1}$					
		I[a]	II	III	IV	V	VI
293	2145	78.32	75.88	76.53			79.21
	1457	52.85	50.12	50.30			49.20
	907	32.66	31.37	31.61			28.12
	494	14.48	17.18	17.22			13.75
308	2130	79.51	76.87	79.20	78.83	75.55	74.47
	1442	57.95	54.63	55.85	54.99	54.52	53.17
	892	33.92	32.58	33.09	32.93	32.38	30.75
	480	18.54	18.00	18.28	18.23	15.56	15.35
318	2113	100.62	88.65	88.81			78.02
	1425	66.05	57.69	57.90			55.63
	875	40.80	35.09	35.75			32.32
	463	24.60	18.64	19.39			18.52
328	2089	109.08	90.18	92.81			84.42
	1401	70.64	59.35	60.16			59.15
	852	45.15	37.63	38.75			34.14
	439	27.61	20.45	21.03			20.31

[a] The systems I–VI are as follows: I, pure methanol; II, methanol containing *o*-nitrophenol (0.36 $mmol \cdot cm^{-3}$); III, methanol containing *o*-nitrophenol (0.18 $mmol \cdot cm^{-3}$) + *o*-aminophenol (0.18 $mmol \cdot cm^{-3}$) + water (0.36 $mmol \cdot cm^{-3}$); IV, methanol containing *o*-aminophenol (0.36 $mmol \cdot cm^{-3}$) + water (0.72 $mmol \cdot cm^{-3}$); V, methanol containing *o*-nitrophenol (0.18 $mmol \cdot cm^{-3}$) + *o*-aminophenol (0.18 $mmol \cdot cm^{-3}$); VI, methanol containing *o*-aminophenol (0.36 $mmol \cdot cm^{-3}$).

The solubility experiments were carried out at least 3 times to ensure reproducibility of the data. All the chemicals used in the solubility measurements were of high-purity grade and they were further purified by fractional distillation or recrystallization.

Results and Discussion

The experimental data on solubility of hydrogen in pure methanol and in the methanol containing *o*-nitrophenol (ONP), *o*-aminophenol (OAP), and water at different pressures and temperatures are presented in Table I. The solubility value was taken as an average of the three replicated data.

Effect of Pressure. The solubility data (Table I) were found to follow the Henry's law

$$S = \alpha p \qquad (1)$$

where S is the solubility of gas, α Henry's constant, and p the gas pressure. The values of Henry's constant, which represents the solubility of H_2 at the pressure of 1 kPa, for the

0021-9568/86/1731-0294$01.50/0

Table II. Values of Henry's Constant (α), Heat of Dissolution (ΔH), and A (Eq 1) for the Dissolution of H_2

system	Henry's constant $\alpha \times 10^3$, μmol·cm^{-3}·kPa^{-1} 293 K	308 K	318 K	328 K	heat of dissoln $-\Delta H \times 10^{-3}$ J·mol^{-1}	A, μmol·cm^{-3}·kPa^{-1}
pure methanol	36.5	40.5	47.5	53.0	−5.01	0.269
ONP (0.36 mmol·cm^{-3}) in methanol	35.0	38.0	41.0	42.5	−8.77	1.32
ONP (0.18 mmol·cm^{-3}) + OAP (0.18 mmol·cm^{-3}) + water (0.36 mmol·cm^{-3}) in methanol	35.0	37.5	41.0	44.25	−5.43	0.324
OAP (0.36 mmol·cm^{-3}) + water (0.77 mmol·cm^{-3}) in methanol		37.0				
ONP (0.18 mmol·cm^{-3} + OAP (0.18 mmol·cm^{-3}) in methanol		35.5				
OAP (0.36 mmol·cm^{-3}) in methanol	33	35	37.25	40.75	−4.93	0.244

Table III. Data on Density of Systems I–VI

temp, K	density, g·cm^{-3} I	II	III	IV	V	VI
293	0.7915	0.8275	0.8087	0.8150	0.8050	0.8025
308	0.7775	0.8017	0.7869	0.7881	0.7835	0.7746
318	0.7696	0.7936	0.7781	0.7793	0.7746	0.7650
328	0.7605	0.7839	0.7695	0.7698	0.7661	0.7548

different systems are given in Table II.

The data on the densities and vapor pressures of the mixed solvents are presented in Tables III and IV, respectively. The former data are measured experimentally. The latter data were obtained from the knowledge of vapor pressures of pure components by applying Raoult's law.

Effect of Temperature. The results in Tables I and II show that, for all the systems, the solubility increases with the increase in the temperature. Figure 1 shows the temperature dependence of Henry's constant for the different systems according to the expression

$$\alpha = A \exp(-\Delta H/RT) \qquad (2)$$

where $-\Delta H$ is the heat of dissolution of gas, R the gas constant, T the temperature, and A a constant. The values of $-\Delta H$ (obtained from the slopes of the linear plots of log α vs. $1/T$, according to eq 2) and A for the different systems are included in Table II. The negative values of the heat of dissolution indicate that the dissolution of H_2 is endothermic for all the systems. This is consistent with the earlier observations (*4*, *5*).

Influence of Reaction Species on the Solubility. It is clear from the results (Tables I and II) that the solubility of H_2 in methanol at all pressures and temperatures is decreased due to the presence of the reaction species in the following order: S(pure methanol) > S[*o*-nitrophenol (0.36 mmol·cm^{-3}) in methanol] > S[*o*-aminophenol (0.36 mmol·cm^{-3}) in methanol].

However, the addition of water to the methanol–OAP and methanol–ONP–OAP systems causes an increase in the solubility. Nevertheless, an addition of either of the reaction species or their mixture reduces the solubility of H_2 in methanol. The increase in the solubility due to the addition of water may probably be due to the interaction of water with the other reaction species.

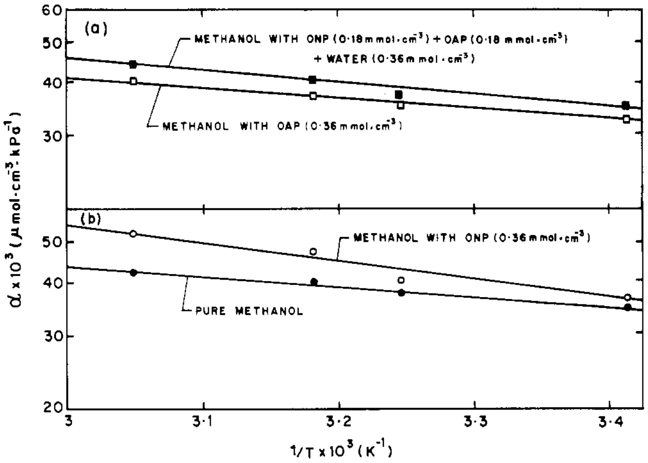

Figure 1. Temperature dependence of Henry's constant for the different systems.

The concentrations of the reaction species in methanol (Table I) for the solubility measurements were chosen considering 0, 50, and 100% conversion of *o*-nitrophenol (initial concentration: 0.36 mmol·cm^{-3}) to *o*-aminophenol in the hydrogenation, so that the variation in the solubility of H_2 in the reaction mixture with the conversion could be followed. The systems II, III, and IV represent the reaction mixture at 0, 50, and 100% conversion of *o*-nitrophenol, respectively.

Glossary

A	constant in eq 2, μmol·cm^{-3}·kPa^{-1}
p	pressure, kPa
R	gas constant, J·mol^{-1}·K^{-1}
S	solubility of gas in liquid, μmol·cm^{-3}
T	temperature, K
α	Henry's constant, μmol·cm^{-3}·kPa^{-1}
$-\Delta H$	heat of dissolution, J·mol^{-1}

Table IV. Data on Vapor Pressure of Systems I–VI

temp, K	component	vapor pressure, kPa I	II	III	IV	V	VI
293	methanol	12.96	12.77	12.57	12.39	12.77	12.77
	o-nitrophenol		0.00024	0.00013		0.00012	
	water			0.0349	0.0675		
308	methanol	27.88	27.46	27.04	26.65	27.46	27.46
	o-nitrophenol		0.00069	0.00035		0.00035	
	water			0.0840	0.1622		
318	methanol	44.42	43.75	43.09	42.47	43.76	43.76
	o-nitrophenol		0.0013	0.00066		0.00067	
	water			0.1434	0.276		
328	methanol	68.57	67.54	66.51	65.55	67.54	67.54
	o-nitrophenol		0.0032	0.0016		0.0015	
	water			0.2354	0.4548		

Registry No. ONP, 88-75-5; OAP, 95-55-6; H_2, 1333-74-0; methanol, 67-56-1; water, 7732-18-5.

Literature Cited

(1) Katayama, T.; Nitta, T. *J. Chem. Eng. Data* **1976**, *21*, 194-196.
(2) Stephen, H.; Stephen, T. *Solubilities of Inorganic and Organic Compounds*; Pergamon: Oxford, U.K., 1963; Vol. I (Part I); p 539-541.
(3) Brahme, P. H.; Vadgaonkar, H. G.; Ozarde, P. S.; Parande, M. G. *J. Chem. Eng. Data* **1982**, *27*, 461-462.
(4) Radhakrishnan, K.; Ramachandran, P. A.; Brahme, P. H.; Chaudhari, R. V. *J. Chem. Eng. Data* **1983**, *28*, 1-4.
(5) Choudhary, V. R.; Choudhari, S. K. *Indian J. Technol.* **1984**, *22*, 156-158.
(6) Choudhary, V. R.; Parande, M. G.; Brahme, P. H.; *Ind. Eng. Chem. Fundam.* **1982**, *21*, 472-474.

Received for review June 6, 1985. Revised manuscript received December 12, 1985. Accepted January 9, 1986.

Gas–Liquid Equilibrium for Ethanol–Water–Carbon Dioxide Mixtures at Elevated Pressures

Michael L. Gilbert and Michael E. Paulaitis*

Department of Chemical Engineering, University of Delaware, Newark, Delaware 19716

Phase compositions for gas–liquid equilibrium have been measured for ternary ethanol–water–CO_2 mixtures at temperatures of 35, 50, and 65 °C and pressures of 10.2, 13.6, and 17.0 MPa. The experimental results can be used to characterize the solvent properties of dense CO_2 in the extraction of ethanol from aqueous solutions.

Introduction

Supercritical or near-critical fluids can be used as solvents for the extraction of organic compounds from aqueous solutions (*1*). One potential application for this solvent extraction technique would be to recover products from fermentation broths. Conventional recovery methods can be prohibitively expensive in these applications since product concentrations are typically quite low. Furthermore, the chemical nature of the products may preclude the use of separations involving distillation or extraction with organic solvents.

In this paper, we present the results of an experimental study of gas–liquid equilibrium at elevated pressures for the ternary system ethanol–water–carbon dioxide. Our results consist of equilibrium phase compositions for the two coexisting fluid phases as a function of temperature and pressure in the vicinity of the critical point of CO_2.

Studies on different aspects of fluid-phase equilibria for ethanol–water–CO_2 mixtures at elevated pressures have been reported previously in the literature. The triangular composition diagram for this ternary mixture at 25 °C and 6.5 MPa has been reported by Francis (*2*). Baker and Anderson (*3*) measured the phase boundary for gas–liquid equilibrium at temperatures from 10 to 50 °C and pressures up to 20 MPa. Although phase boundaries were determined with only moderate accuracy, the extent of the two-phase region on triangular composition diagrams was observed to initially decrease and then increase with increasing temperature at constant pressure. Their results also show that ethanol extraction with compressed CO_2 as the solvent will not give alcohol concentrations greater than that corresponding to the ethanol–water azeotrope. Efremova and Shvarts (*4*, *5*) measured gas–liquid and liquid–liquid critical end points which bound three-phase, gas–liquid–liquid equilibrium. They observed a tricritical point at 47.4 °C and 9.17 MPa where the gas–liquid and liquid–liquid critical end-point curves intersect. Kuk and Montagna (*6*) measured both CO_2 solubilities in ethanol–water mixtures and ethanol–water solubilities in compressed CO_2 at 40 and 60 °C, elevated pressures, and various ethanol concentrations. The reported results can be used to construct the phase boundary for gas–liquid equilibrium, but cannot be used to generate equilibrium tie-line compositions for this ternary system.

Experimental Section

A schematic diagram of the experimental apparatus is presented in Figure 1. A flow technique is used to facilitate mixing and subsequent sampling of the two fluid phases at elevated pressures. Liquid CO_2 and the ethanol–water solution are compressed to the desired operating pressure and delivered by separate high-pressure, liquid feed pumps (Milton Roy Model 396-89). These pumps are rated to 40 MPa and can operate over a range of flow rates from 46 to 460 mL/h. Typical flow rates for both pumps were on the order of 5 g/min.

After exiting the feed pumps, the two streams are combined and heated to the desired operating temperature in the crimped preheat line within the constant temperature bath. The equilibrated mixture then enters the view cell (Jerguson sight gauge, Model 17-T-40) where the two equilibrium phases separate. The more dense, liquid phase flows out the bottom of the view cell and is flashed to atmospheric pressure across the back pressure regulator (Grove Model 5-91 XW). The condensed portion of this sample is trapped in a dry ice–acetone bath while the CO_2 volume is measured by passing the gas through a wet-test meter (Precision Scientific Co.). The trapped condensate is subsequently weighed and analyzed by standard gas chromatographic techniques. The less dense fluid phase flows out the top of the view cell and is flashed across the heated micrometering valve (Whitey Co.). This two-phase sample is then analyzed by the same procedure described above for the dense, liquid phase.

The operating pressure of the system is set and maintained with the back pressure regulator, while the liquid level in the view cell is controlled by visually monitoring the gas–liquid meniscus and adjusting the micrometering valve to maintain two phases within the cell. System pressure is measured with a Bourdon-type Heise gauge (Gregory Model CM, 0-5000 psi range) accurate to ±0.05 MPa. Pressure variations due to pumping were found to be less than ±0.167 MPa over the entire pressure range studied, and were typically less than ±0.10 MPa. System temperature is controlled to within ±0.15 °C with a Sargent-Welch Thermonitor, and is measured to

0021-9568/86/1731-0296$01.50/0